Glutamate is an inhibitory neurotransmitter in the *Drosophila* olfactory system

Wendy W. Liu and Rachel I. Wilson[1]

Department of Neurobiology, Harvard Medical School, Boston, MA 02115

Edited by Liqun Luo, Stanford University, Stanford, CA, and approved March 28, 2013 (received for review November 30, 2012)

Glutamatergic neurons are abundant in the *Drosophila* central nervous system, but their physiological effects are largely unknown. In this study, we investigated the effects of glutamate in the *Drosophila* antennal lobe, the first relay in the olfactory system and a model circuit for understanding olfactory processing. In the antennal lobe, one-third of local neurons are glutamatergic. Using in vivo whole-cell patch clamp recordings, we found that many glutamatergic local neurons are broadly tuned to odors. Iontophoresed glutamate hyperpolarizes all major cell types in the antennal lobe, and this effect is blocked by picrotoxin or by transgenic RNAi-mediated knockdown of the *GluClα* gene, which encodes a glutamate-gated chloride channel. Moreover, antennal lobe neurons are inhibited by selective activation of glutamatergic local neurons using a nonnative genetically encoded cation channel. Finally, transgenic knockdown of *GluClα* in principal neurons disinhibits the odor responses of these neurons. Thus, glutamate acts as an inhibitory neurotransmitter in the antennal lobe, broadly similar to the role of GABA in this circuit. However, because glutamate release is concentrated between glomeruli, whereas GABA release is concentrated within glomeruli, these neurotransmitters may act on different spatial and temporal scales. Thus, the existence of two parallel inhibitory transmitter systems may increase the range and flexibility of synaptic inhibition.

interneuron | olfaction | glomerulus | VGlut | volume transmission

Identifying the physiological effects of neurotransmitters is critical to deciphering neural circuit function. In the vertebrate central nervous system (CNS), glutamate serves as the major excitatory neurotransmitter, whereas GABA and glycine serve as the major inhibitory neurotransmitters. Like the vertebrate CNS, the *Drosophila* CNS uses several major neurotransmitters: Acetylcholine is the major fast excitatory neurotransmitter, and GABA is the major fast inhibitory neurotransmitter. Recent studies have demonstrated that glutamatergic neurons are widespread in the *Drosophila* CNS (1, 2), but its effects are poorly understood. Much attention has been focused on the idea that the effects of glutamate in the *Drosophila* CNS are excitatory (3–8). However, this idea has remained largely untested. There are 30 putative ionotropic glutamate receptor subunits in the *Drosophila* genome. Most are homologous to mammalian AMPA/kainate and NMDA receptors (9), but the genome also contains a metabotropic glutamate receptor (10) and a glutamate-gated chloride channel (11), suggesting that glutamate can have a variety of physiological effects.

Much of what we know about synaptic physiology in the *Drosophila* CNS comes from studies of the antennal lobe. The antennal lobe is one of the most well-studied regions of the fly brain, and because it bears some homology to the vertebrate olfactory bulb, it has been a model for understanding olfactory processing (12, 13). Roughly one-third of antennal lobe local neurons (LNs) are immunopositive for the vesicular glutamate transporter (60–70 of ∼200 total LNs); these cells are also immunonegative for GABA, unlike most LNs (8, 14). These observations imply a major role for glutamate in this neural circuit. There is evidence for several glutamate receptors in the antennal lobe, including NMDA receptors (3–5) and metabotropic glutamate receptors (15, 16). Knocking down NMDA receptor expression specifically in antennal lobe projection neurons interferes with olfactory habituation (3, 4). However, the effects of glutamate have not been characterized in this circuit. In this study, we investigated the effect of glutamate on antennal lobe neurons and also the functional role of glutamatergic neurons in olfactory processing.

Results

Glutamate Release Is Concentrated in the Interglomerular Space. The antennal lobe is divided into ∼50 glomeruli (Fig. 1*A*), with each glomerulus corresponding to a different type of olfactory receptor neuron (ORN). Antennal lobe LNs interconnect glomeruli via dendrodendritic synapses onto projection neurons (PNs), and/or dendroaxonic synapses onto ORNs. Previous studies have shown that some antennal lobe LNs are immunopositive for the vesicular glutamate transporter (VGlut) and immunonegative for GABA (8, 14). These neurons have somata that are ventral to the antennal lobe and are labeled by the *OK371-Gal4* line (Fig. 1 *B* and *C*).

In the neuropil, we noticed that VGlut is concentrated primarily in the spaces between glomeruli and is only sparsely present inside glomeruli (Fig. 1*D*). This pattern contrasts with that of the vesicular GABA transporter, which is densely and fairly uniformly expressed throughout the antennal lobe neuropil (Fig. 1*E*). This observation suggests that glutamate and GABA act differently within the antennal lobe.

Glutamatergic LNs Have Diverse Morphologies and Odor Responses. Next, we performed in vivo whole-cell recordings to characterize glutamatergic LNs (Glu-LNs). We used GFP to target our electrodes to Glu-LNs, and we filled cells with biocytin via the patch pipette. We observed that these neurons have diverse morphologies, consistent with previous reports (8, 14), and also diverse physiological properties.

One morphological class of Glu-LNs innervated many glomeruli (Fig. 2*A*). These neurons were broadly tuned to odors (Fig. 2 *B* and *C*). A second class of Glu-LNs had more selective innervation patterns, generally projecting to one ventral glomerulus (Fig. 2*D*). Some of the ORNs innervating this region are narrowly tuned to organic acids (17). Accordingly, some Glu-LNs with this innervation pattern responded preferentially to the organic acid in our test set (butyric acid), although most were broadly tuned (Fig. 2 *E* and *F*). A third class of Glu-LNs sent only sparse projections to olfactory glomeruli and, instead, densely innervated the region just posterior to olfactory glomeruli (Fig. 2*G*). This region contains several glomeruli that receive input from hygrosensitive and thermosensitive neurons in the arista (18). These Glu-LNs typically responded more strongly to water vapor than to odors (Fig. 2 *H* and *I*).

These data indicate that Glu-LNs constitute a diverse population of neurons. Nonetheless, most Glu-LNs are broadly tuned, and so most stimuli will recruit many Glu-LNs, raising the issue of how glutamate affects other neurons in the antennal lobe.

Author contributions: W.W.L. and R.I.W. designed research; W.W.L. performed research; W.W.L. analyzed data; and W.W.L. and R.I.W. wrote the paper.

The authors declare no conflict of interest.

This article is a PNAS Direct Submission.

Freely available online through the PNAS open access option.

[1]To whom correspondence should be addressed. E-mail: rachel_wilson@hms.harvard.edu.

This article contains supporting information online at www.pnas.org/lookup/suppl/doi:10.1073/pnas.1220560110/-/DCSupplemental.

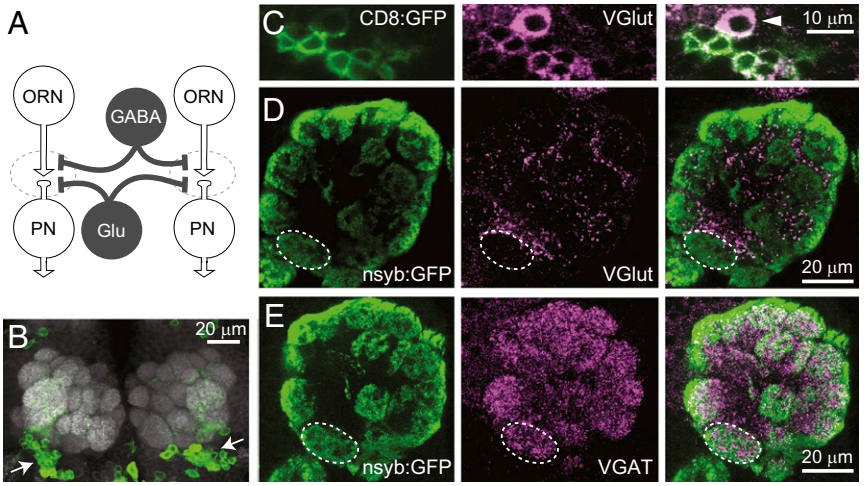

Fig. 1. Glutamatergic LNs in the antennal lobe. (*A*) Schematic of the antennal lobe circuit. Excitatory neurons are in white, and LNs are in gray. Dashed lines encircle glomeruli. Some cell types and connections are omitted for clarity. (*B*) Confocal immunofluorescence image of the *Drosophila* brain. Neuropil is labeled with nc82 antibody (white), and cells that express Gal4 under the control of *OK371-Gal4* are labeled with CD8:GFP (green). The somata of Glu-LNs are clustered ventral to the antennal lobes (arrows). Image is a *z*-projection of coronal optical slices through a 27-μm depth. (*C*) GFP+ neurons are immunopositive for VGluT (see also ref. 8). Image is a 1-μm confocal slice through one of the clusters of Glu-LN somata shown in *B*. Note that some $VGluT^+$ somata are not GFP^+ (arrowhead). (*D*) Coronal optical section through one antennal lobe, with glomerular compartments indicated by a presynaptic marker (nsyb:GFP) expressed specifically in ORNs. One glomerulus (VM4, dashed lines) is outlined as a landmark. (*E*) Same as *D* but with staining for the vesicular GABA transporter (VGAT).

Glutamate Hyperpolarizes PNs and GABAergic LNs via a Glutamate-Gated Chloride Channel. Next, we asked how exogenous glutamate affects antennal lobe neurons. We performed in vivo whole cell recordings from the somata of PNs and GABAergic LNs (GABA-LNs), using microiontophoresis to apply brief pulses of glutamate into the antennal lobe neuropil. Glutamate consistently hyperpolarized both PNs and GABA-LNs (Fig. 3*A*).

Most of the glutamate response was blocked by bath-applied picrotoxin (100 μM), and the effect of picrotoxin was similar in PNs and GABA-LNs (Fig. 3 *A* and *C*). Picrotoxin is a broad-spectrum chloride channel pore blocker, and although it is most commonly used as a $GABA_A$ antagonist, it can also block GluCl homomers (19). In some experiments, we observed that picrotoxin's effect was incomplete, which is consistent with the properties of glutamate-gated chloride conductances in other species (20, 21). The concentration of picrotoxin we needed to achieve this level of blockade was higher than that needed to block GABA-gated chloride conductances in the same neurons (22), but we were not able to find a picrotoxin concentration that would completely block GABA-gated conductances without affecting glutamate-gated conductances.

To test whether the glutamate-gated conductance in antennal lobe neurons requires the *GluClα* gene, we used Gal4/UAS to express an RNAi hairpin targeting *GluClα* specifically in antennal lobe PNs, and we coexpressed GFP in these neurons to mark them for recording. In control experiments, the RNAi hairpin transgene was omitted. We found that *GluClα* knockdown virtually abolished the response to iontophoresed glutamate (Fig. 3 *D* and *E*). As a control, we verified that *GluClα* knockdown did not reduce responses to GABA-gated currents in PNs (Fig. S1).

We never observed a depolarizing response to glutamate in these recordings, when picrotoxin was present or when *GluClα* expression was knocked down. Moreover, the ionotropic glutamate receptor antagonists 6-cyano-7-nitroquinoxaline-2,3-dione [(CNQX) 10 μM] and MK801 (100 μM) had no effect on the response to iontophoresed glutamate. The metabotropic glutamate receptor antagonist LY341495 (1 μM) also had no effect.

Glutamatergic LNs Inhibit PNs. We next investigated the effects of endogenous glutamate on antennal lobe PNs. To selectively stimulate glutamatergic LNs, we misexpressed an ATP-gated cation channel (P2X2) under the control of *OK371-Gal4*. Because there are no native *Drosophila* channels gated by ATP (9), applying ATP should selectively depolarize the neurons that express Gal4 (23). In these experiments, we also coexpressed GFP with P2X2 to mark these neurons. As expected, Glu-LNs were depolarized by a brief ATP pressure ejection (Fig. 4*A*), but only when the Gal4 transgene was present (*SI Methods*). We estimate that several dozen Glu-LNs are being depolarized simultaneously by this stimulus.

We found that PNs were inhibited by selectively stimulating Glu-LNs. Specifically, in whole-cell recordings from PNs, the membrane potential was hyperpolarized and spontaneous spiking

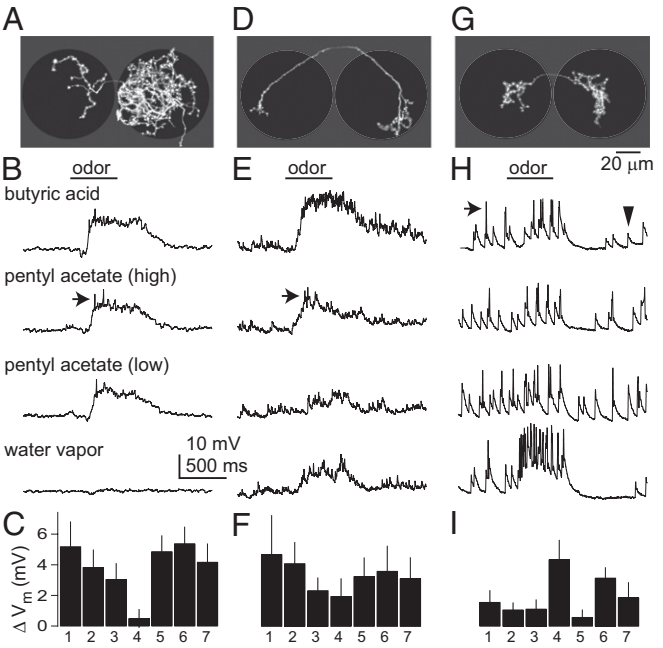

Fig. 2. Morphology and physiology of Glu-LNs. (*A*) Morphology of a Glu-LN, shown as a *z*-projection of a traced biocytin fill. This neuron innervated many olfactory glomeruli, and this pattern was seen in 11 of 29 filled cells. Note innervation of both antennal lobes (black circles), which is typical of Glu-LNs. (*B*) A whole-cell current clamp recording from a Glu-LN of this morphological type. The spikes fired by this cell (arrow) are small. (*C*) Mean responses of all of the Glu-LNs of this type (±SEM across experiments), quantified as the change in membrane potential averaged over the stimulus period. Odors are 1, butyric acid; 2, pentyl acetate (10^{-2}); 3, pentyl acetate (10^{-6}); 4, water; 5, methyl benzoate; 6, 1-butanol; 7, ethyl acetate. (*D*) This neuron innervated mainly a single ventral olfactory glomerulus on both sides of the brain. A similar pattern was seen in 8 of 29 fills. (*E*) A recording from this type of neuron. Spikes (arrow) are small. (*F*) Mean responses for all of the Glu-LNs of this type. (*G*) This neuron innervated the putative hygrosensitive/thermosensitive glomeruli just posterior to the antennal lobe. A similar pattern was seen in 10 of 29 fills. (*H*) A recording from this type of neuron. Note prominent spikes (arrow) and large excitatory postsynaptic potentials (arrowhead). (*I*) Mean responses for all of the Glu-LNs of this type.

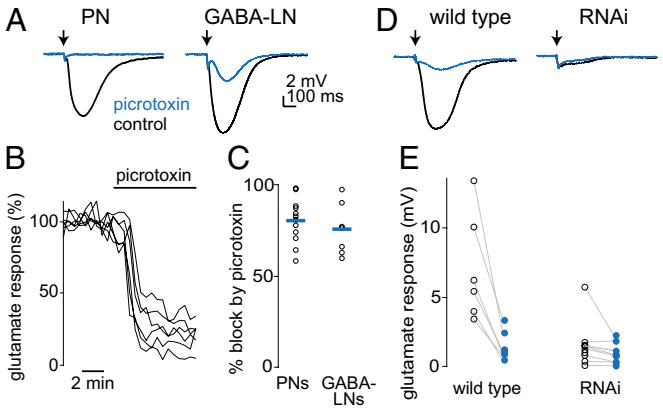

Fig. 3. *GluClα* mediates a glutamate-gated chloride conductance in PNs and GABAergic LNs. (*A*) Whole-cell current-clamp recording from the soma of an antennal lobe PN (*Left*) and a GABA-LN (*Right*). A pulse of glutamate in the antennal lobe neuropil (arrow, 10–20 ms) hyperpolarizes both cells. Picrotoxin (100 μM) either abolishes or attenuates the response, depending on the recording. (*B*) Time course of the effect of picrotoxin on glutamate responses in PNs. Each line is a different PN recording. (*C*) Effect of picrotoxin on responses to glutamate. Each symbol is a different recording, with means in blue. Overall, the effects of picrotoxin were similar in PNs ($n = 12$) and GABA-LNs ($n = 7$). (*D*) Responses to glutamate before and after applying 100 μM picrotoxin in a wild-type PN (*Left*) and a PN expressing *GluClα* RNAi (*Right*). Arrow indicates iontophoretic pulses. The residual deflection is a stimulus artifact. (*E*) Hyperpolarizing responses to iontophoresis in both genotypes, before picrotoxin (black) and after picrotoxin (blue). The response to glutamate is significantly smaller in RNAi flies versus wild type ($P < 0.05$, Student's *t* test, $n = 6$ wild type and 9 RNAi). The percent inhibition by picrotoxin is also significantly smaller ($P < 0.0001$, Student's *t* test).

was paused (Fig. 4 *B–D*). These effects were blocked by picrotoxin (Fig. 4 *B* and *E*). As a control, we verified that these effects were absent when the Gal4 transgene was omitted (*SI Methods*).

For comparison, we used the same technique to selectively stimulate GABA-LNs. We expressed P2X2 in a large population of GABA-LNs under the control of *NP3056-Gal4*, and we verified that ATP depolarizes these neurons (Fig. 4*F*). We found that GABA-LNs and Glu-LNs had similar effects on PNs; specifically, the membrane potential was hyperpolarized and spiking was paused (Fig. 4 *G–I*). As expected, inhibition by GABA-LNs was blocked by the $GABA_A$ antagonist picrotoxin and the $GABA_B$ antagonist CGP54626 (Fig. 4*J*).

Together, these results indicate that Glu-LNs can inhibit PNs, similar to the effects of GABA-LNs on PNs. Although glutamate release is not concentrated within glomeruli, coactivation of multiple Glu-LNs is sufficient to produce robust effects on PNs, possibly due to pooling of glutamate from multiple LNs.

Glutamatergic LNs Inhibit GABAergic LNs. We next asked whether Glu-LNs can inhibit GABA-LNs. This experiment was motivated by our observation that iontophoresed glutamate hyperpolarizes GABA-LNs (Fig. 3). As before, we drove P2X2 expression specifically in Glu-LNs, and we stimulated Glu-LNs with ATP. Recordings from GABA-LNs showed that they were hyperpolarized and spontaneous firing was suppressed (Fig. 5 *A–C*). These effects were abolished by picrotoxin (Fig. 5*D*).

We then repeated this experiment, but this time stimulating GABA-LNs rather than Glu-LNs. As in all these experiments, we coexpressed GFP with P2X2, and we could identify non–P2X2-expressing cells by their lack of GFP expression. We could therefore stimulate some GABA-LNs while recording from other GABA-LNs that were not directly stimulated. These recordings showed robust inhibition (Fig. 5 *E–G*), which was blocked by picrotoxin and CGP54626 (Fig. 5*H*).

Thus, GABA-LNs receive inhibition from both Glu-LNs and other GABA-LNs, providing further evidence that glutamate and GABA function in parallel as inhibitory neurotransmitters.

Paired Recordings Reveal Connections Made by Individual Glutamatergic and GABAergic Neurons. We next used paired whole-cell recordings to investigate the connectivity of individual LNs. In every paired recording, we injected depolarizing current into one cell while monitoring the response of the nonstimulated cell. LNs do not have axons, and PNs do not make axonal synapses in the antennal lobe, and so connections between these neurons must represent dendrodendritic interactions.

In these recordings, the highest rate of connectivity was observed between GABA-LNs and PNs. In most cases, depolarizing the GABA-LN hyperpolarized the PN (Fig. 6*A*), and these responses were abolished by CGP54626. In most cases, these connections were reciprocal: Depolarizing the PN depolarized the GABA-LN (Fig. 6*B*). These connections were blocked by the nicotinic antagonist mecamylamine, consistent with the fact that PNs are cholinergic (24).

Next, we performed paired recordings from Glu-LNs and PNs (Fig. 6 *C* and *D*). We did not detect any connections from Glu-LNs onto PNs in 65 pairs, which is significantly different from the connection rate in paired recordings with GABA-LNs and PNs ($P < 0.001$; two-sample binomial test). Our failure to detect these connections is difficult to explain by postulating a low rate of connectivity: Even if each PN received input from only 5 of the ~70 Glu-LNs, obtaining 0 hits in 65 attempts is improbable

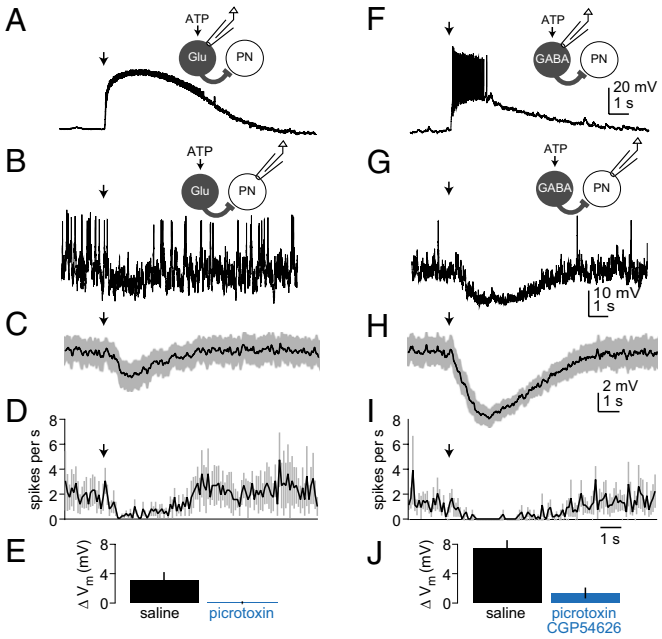

Fig. 4. PNs are inhibited by stimulation of either Glu-LNs or GABA-LNs. (*A*) A recording from a P2X2-expressing Glu-LN, showing that ATP ejection (arrow) depolarized the cell and elicited a train of small spikes. (*B*) A recording from a PN showing that, when Glu-LNs were stimulated with ATP (arrow), spontaneous spiking paused, and the membrane was slightly hyperpolarized. (*C*) Mean membrane potential of PNs in response to Glu-LN stimulation, averaged across experiments, ±SEM ($n = 13$). (*D*) Mean firing rate of PNs in response to Glu-LN stimulation, averaged across experiments, ±SEM ($n = 9$; some cells were excluded because they did not spike during the analysis window). (*E*) Mean membrane potential change of PNs in response to Glu-LN stimulation, averaged across experiments, ±SEM. Picrotoxin significantly reduced the response to Glu-LN stimulation ($P < 0.05$, paired *t* test, $n = 4$). (*F–J*) Same as above, but this time stimulating GABA-LNs rather than Glu-LNs ($n = 13$ for *H* and *J*, and $n = 9$ for *I*). Picrotoxin (5 μM) and CGP54626 (50 μM) significantly reduced the membrane potential change in response to GABA-LN stimulation ($P = 0.01$, paired *t* test, $n = 8$).

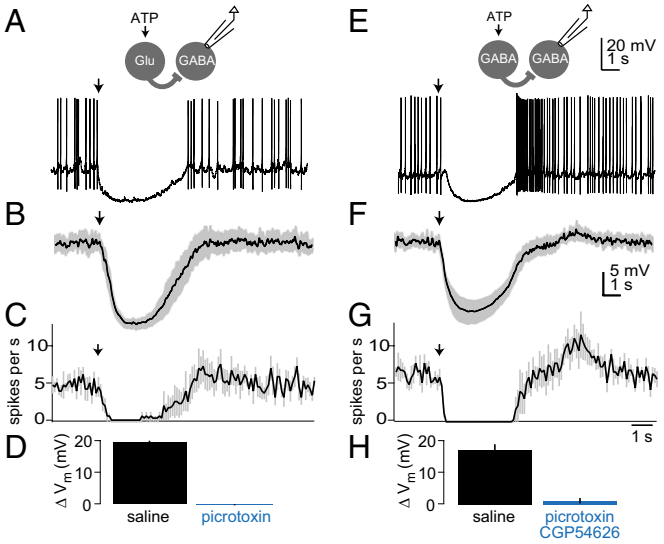

Fig. 5. GABA-LNs are inhibited by stimulation of either Glu-LNs or GABA-LNs. (*A*) A GABA-LN recording. When Glu-LNs were stimulated with ATP (arrow), spontaneous spiking paused and the membrane potential hyperpolarized. (*B*) Mean membrane potential of GABA-LNs in response to Glu-LN stimulation, averaged across experiments, ±SEM ($n = 6$). (*C*) Mean firing rate of GABA-LNs in response to Glu-LN stimulation, averaged across experiments, ±SEM ($n = 6$). (*D*) Mean membrane potential change of GABA-LNs in response to Glu-LN stimulation, averaged across experiments, ±SEM. Picrotoxin significantly reduced the response to Glu-LN stimulation ($P < 0.001$, paired *t* test, $n = 4$). (*E–H*) Same as above, but this time stimulating GABA-LNs rather than Glu-LNs. Picrotoxin (100 μM) and CGP54626 (50 μM) significantly reduced the response to GABA-LN stimulation ($P = 0.001$, paired *t* test, $n = 5$). Although GABA-LNs lack $GABA_B$ conductances (22), CGP54626 was needed to produce complete block; GABA-LN stimulation may inhibit tonically active ORNs and PNs via both $GABA_A$ and $GABA_B$ receptors, thereby reducing tonic excitation to GABA-LNs.

($P < 0.01$, binomial test). This result suggests that multiple Glu-LNs must be coactivated to inhibit a PN, which could indicate that glutamate must diffuse some distance before acting on PNs.

Our results were similar when we probed for connections in the other direction, from PNs onto Glu-LNs. Consistent with the idea that PNs and Glu-LNs are generally not in direct contact, we observed no connections except in two isolated cases. In one case, depolarizing the PN produced a depolarization in the Glu-LN, which was blocked by the nicotinic antagonist mecamylamine. In the other case, we observed hyperpolarization which was blocked by the muscarinic antagonist atropine.

Finally, we performed paired recordings from Glu-LNs and GABA-LNs. In several of these pairs, depolarizing the Glu-LN elicited a hyperpolarization in the GABA-LN (Fig. 6*E*), which was blocked by picrotoxin. Conversely, depolarizing the GABA-LN elicited a hyperpolarization in the Glu-LN in several of the pairs we recorded from (Fig. 6*F*), which was also blocked by picrotoxin. These data show that individual Glu-LNs and GABAergic LNs can mutually inhibit each other.

Eliminating Glutamatergic Inhibition in PNs Disinhibits Odor Responses. Finally, we asked whether knocking down *GluClα* expression in PNs alters PN odor responses. Gal4/UAS was used to express an RNAi hairpin against *GluClα* specifically in antennal lobe PNs, and GFP was coexpressed in these neurons to mark them for recording. In control experiments, the RNAi hairpin transgene was omitted. We filled each recorded PN with biocytin and used post hoc confocal microscopy to identify the glomerulus it innervated.

We recorded from 29 PNs in total in these experiments. Four different glomeruli appeared in both the control dataset and the RNAi dataset. Because different glomeruli have diverse odor responses, meaningful between-experiment comparisons can only be made by comparing results within a glomerulus. Therefore, we analyzed only the four PN types corresponding to the four glomeruli that appeared in both datasets: DL1, VM2, VM5, and VA1v.

Knocking down *GluClα* in these PNs systematically disinhibited all odor responses (Fig. 7 *A* and *B*). Odor-evoked excitatory responses were increased, and in one PN type (VA1v), odor-evoked inhibition was converted to odor-evoked excitation (Fig. 7 *C* and *D*). These results demonstrate that glutamatergic inhibition makes a measurable contribution to the output of the antennal lobe, and that its direct effect on PNs is inhibitory.

Discussion

Glutamate as an Inhibitory Neurotransmitter Acting via GluClα. Although glutamatergic neurons are abundant in the *Drosophila* brain (1), the role of glutamate as a neurotransmitter in the *Drosophila* CNS has received little study. In the antennal lobe, where approximately one-third of LNs are glutamatergic (8, 14), the physiological effects of glutamate have never been characterized. In this study, we show that glutamate is an inhibitory transmitter that shapes the responses of PNs to olfactory stimuli.

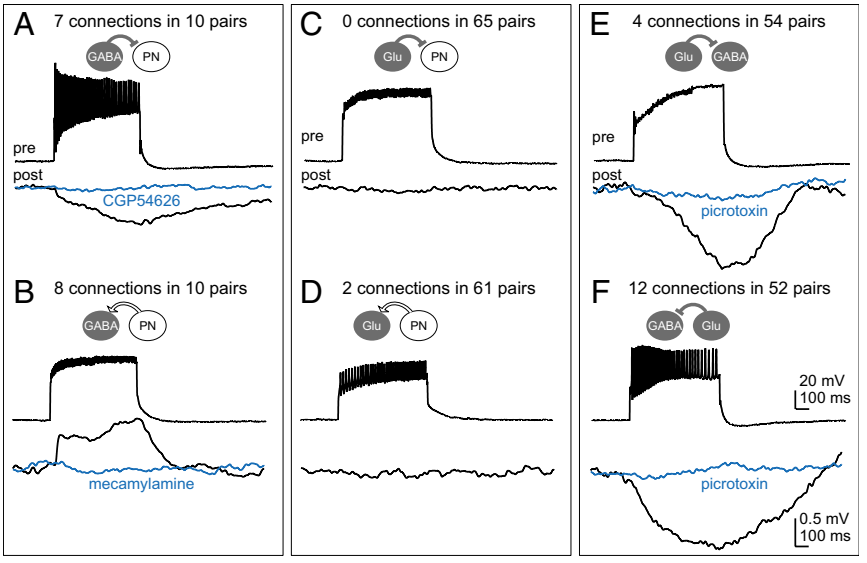

Fig. 6. Paired recordings reveal the connectivity of individual LNs. (*A*) An example of an inhibitory connection from a GABA-LN onto a PN. Depolarizing current was injected into the GABA-LN through the patch electrode (pre, single trial). CGP54626 (50 μM) blocked the response in the PN (post, mean of 50–60 trials). (*B*) An example of an excitatory connection from a PN onto a GABA-LN. Mecamylamine (50 μM) blocked the response. Scale bars apply to all graphs. (*C*) In a typical paired recording, there was no effect of stimulating a Glu-LN on a PN. (*D*) Similarly, in the same pair, there was no effect of stimulating the PN on the Glu-LN. The total number of pairs tested is not identical to *C* because a few recordings were lost before both directions of connectivity could be tested. (*E*) An example of an inhibitory connection from a Glu-LN onto a GABA-LN. Note that the presynaptic spikes are very small, which is typical of many Glu-LNs. Picrotoxin (100 μM) blocked the response. (*F*) An example of an inhibitory connection from a GABA-LN onto a Glu-LN. Picrotoxin (5 μM) blocked the response.

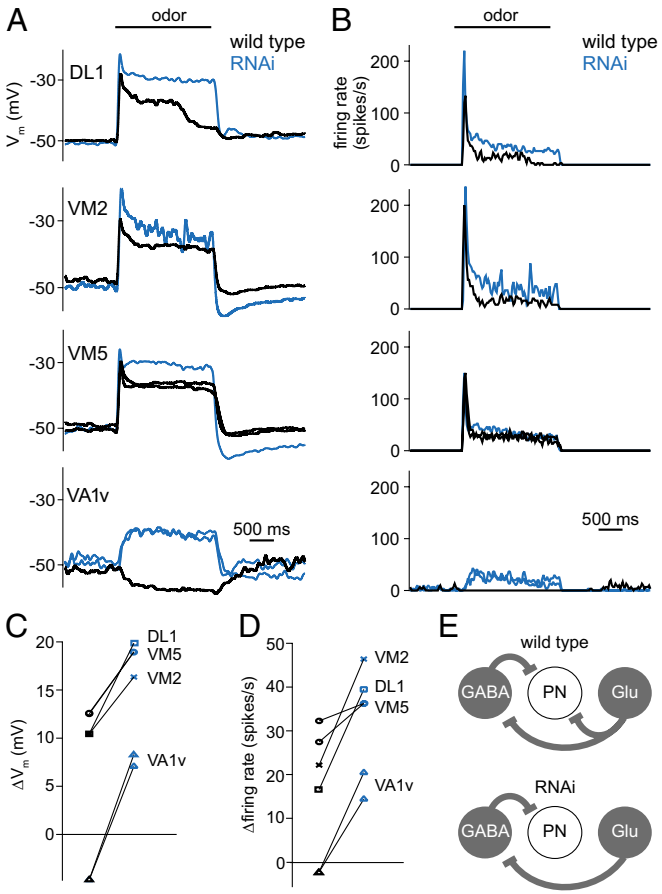

Fig. 7. Odor responses are disinhibited by knockdown of *GluClα* in PNs. (*A*) Odor responses of PNs in four different glomeruli. The membrane potential is low-pass filtered to remove spikes. Each trace represents a different recording, with 10 PNs total. In half of these experiments (blue traces), we used transgenic RNAi to knock down *GluClα* expression specifically in PNs. Black traces are wild type. Responses are averaged across 5–6 trials. Odor stimuli are pentyl acetate (10^{-2} dilution; VM2, VM5, VA1v) and methyl salicylate (10^{-2} dilution; DL1). (*B*) Peristimulus time histograms showing spiking responses of the same PNs. (*C*) Mean odor-evoked changes in membrane potential (averaged over the 2-s stimulus period) in all cells. Each symbol represents a different recording ($n = 5$ control, $n = 5$ RNAi). Responses in wild-type (black) and RNAi flies (blue) are significantly different ($P < 0.001$, two-way ANOVA). The values for the two wild-type VM5 recordings are so similar that their symbols lie on top of one another. (*D*) Mean odor-evoked firing rates for the same cells. Responses in wild-type and RNAi flies are significantly different ($P < 0.005$, two-way ANOVA). (*E*) Schematic showing interactions between PNs, and LNs in the two genotypes. Some connections are omitted for clarity.

In the past, glutamate has been proposed to mediate lateral excitation between olfactory glomeruli (8). Our results demonstrate that the main effect of glutamate is inhibition, not excitation. We cannot rule out the possibility that glutamate has small excitatory effects, but we could not find evidence of excitation even when *GluClα* was knocked down genetically or inhibited pharmacologically. We note that there is in fact lateral excitation in the antennal lobe, which exists in parallel with lateral inhibition (25, 26). However, lateral excitation is mediated not by glutamate, but by electrical coupling between LNs and PNs (24, 27).

We found that all of the effects of glutamate on PNs were eliminated by knocking down *GluClα*. The dominant role for *GluClα* is notable, given how many other glutamate receptors are in the genome. Our results are particularly surprising in light of two recent studies that have reported behavioral effects of knocking down an NMDA receptor subunit (*NR1*) in PNs (3, 4). Further experiments will be needed to clarify the role of *NR1*.

There is a precedent for the idea that glutamate can be an inhibitory neurotransmitter in the *Drosophila* brain. Specifically, several studies have reported that bath-applied glutamate inhibits the large ventrolateral neurons of the *Drosophila* circadian clock circuit (28–30). Collectively, these studies suggest roles for both ionotropic and metabotropic glutamate receptors in glutamatergic inhibition. Regardless of which glutamate receptors are involved, these studies are consistent with the conclusion that glutamate is an important mediator of synaptic inhibition.

The idea that glutamate can be inhibitory has important implications for neural coding. One particularly interesting case is the motion vision circuit of the *Drosophila* optic lobe. Two neuron types, L1 and L2, both receive strong synaptic inputs from photoreceptors, and they respond equally to contrast increments ("on") and decrements ("off") (31). However, based on conditional silencing experiments, L1 is thought to provide input to an on pathway, and L2 to an off pathway (32). Therefore, opponency must arise downstream from L1 and L2 (31, 32). According to recent evidence, L1 is glutamatergic, whereas L2 is cholinergic (33). In light of our data, that result suggests that L1 may actually be inhibitory, which would be sufficient to create opponency in the on and off pathways.

Glutamate can act as an inhibitory neurotransmitter in the *Caenorhabditis elegans* olfactory circuit, and this fact too has implications for neural coding of odors in this organism. In the worm, a specific type of glutamatergic olfactory neuron inhibits one postsynaptic neuron via GluCl, while also exciting another postsynaptic neuron via an AMPA-like receptor. This arrangement creates a pair of opponent neural channels that respond in an anticorrelated fashion to odor presentation or odor removal (34), analogous to opponent channels in the visual system.

Comparisons Between Glutamatergic and GABAergic Inhibition. We have shown that the cellular actions of Glu-LNs are broadly similar to the actions of GABA-LNs. Specifically, both types of LNs inhibit PNs and other LNs. In addition, we found that both GABA and glutamate inhibit neurotransmitter release from ORNs (Fig. S2). Thus, both neurotransmitters inhibit all of the major cell types in the antennal lobe circuit.

However, Glu-LNs and GABA-LNs are not functionally identical. In particular, we found that the vesicular glutamate transporter is mainly confined to the spaces between glomeruli, whereas the vesicular GABA transporter is abundant within glomeruli. This finding implies that glutamate and GABA are released in largely distinct spatial locations. Consistent with this implication, we observed no individual synaptic connections from Glu-LNs onto PNs, whereas we observed a substantial rate of connections from GABA-LNs onto PNs. Nevertheless, we found that PNs are hyperpolarized by coactivation of multiple Glu-LNs, and PNs are disinhibited by knockdown of GluCl specifically in PNs.

These results can be reconciled by a model where the sites of glutamate release are distant from PN glutamate receptors. As a result, glutamate would need to diffuse some distance to inhibit PNs. Coactivation of multiple Glu-LNs would increase extracellular glutamate concentrations, overwhelming uptake mechanisms and allowing glutamate to diffuse further. In this scenario, glutamatergic inhibition should be most important when LN activity is intense and synchronous. By comparison, GABAergic inhibition of PNs does not require LN coactivation, implying a comparatively short distance between presynaptic and postsynaptic sites. There is a precedent in the literature for the idea that different forms of inhibition can be differentially sensitive to LN coactivation, due to the spatial relationship between presynaptic and postsynaptic sites. In the hippocampus, $GABA_A$ receptors are closer than $GABA_B$ receptors to sites of GABA release, and so activation of individual interneurons produces $GABA_A$ but not $GABA_B$ currents, whereas coactivation of many interneurons produces both $GABA_A$ and $GABA_B$ currents (35).

The pharmacology of glutamate-gated conductances in antennal lobe neurons is similar to the pharmacology of $GABA_A$ conductances in these neurons. This result should prompt a

reevaluation of studies that used picrotoxin to block inhibition in the antennal lobe (22, 36–40). Given our results, it seems likely that these studies were reducing both glutamatergic and GABAergic inhibition.

Interactions Between Glutamatergic and GABAergic Inhibition. It is perhaps surprising that knocking down *GluClα* in PNs had such a substantial effect on PN odor responses, given that picrotoxin alone has comparatively modest effects (22, 36–39). The solution to this puzzle may lie in our finding that glutamate regulates not only PNs but also GABA-LNs. Importantly, GABA-LNs are spontaneously active and provide tonic inhibition to PNs (14, 22). Hence, in the intact circuit, glutamatergic inhibition of GABA-LNs should tend to disinhibit PNs (Fig. 7*E*). Picrotoxin prevents Glu-LNs from inhibiting GABA-LNs and should tend to potentiate GABAergic inhibition. The effects of GABA are mediated in part by $GABA_B$ receptors, which are not sensitive to picrotoxin. Thus, picrotoxin likely has bidirectional effects on the total level of inhibition in the circuit. By contrast, knockdown of *GluClα* specifically in PNs should not directly affect GABA-LNs and should not produce these complex effects (Fig. 7*E*). These results illustrate how a cell-specific genetic blockade of a neurotransmitter system can have more dramatic effects than a global pharmacological blockade of the same system.

Our study reveals that an LN can have push-pull effects on a single population of target cells. For example, Glu-LNs directly inhibit PNs, but they should also disinhibit PNs, via the inhibition of GABA-LNs. This architecture may allow for more robust gain control and rapid transitions between network states and is similar to the wiring of many cortical circuits, where corecruitment of excitation and inhibition is a common motif (41).

Why might the existence of two parallel inhibitory transmitters be useful? Our data argue that GABA and glutamate may act on different spatial and temporal scales. Because these two inhibitory systems comprise different cells, receptors, and transporters, they can be modulated independently. Because their properties are encoded by different genes, they can also evolve independently. This organization should confer increased flexibility in adapting synaptic inhibition to a changing environment.

Methods

Immunohistochemical procedures, in vivo whole-cell recordings, odor stimulation, and antennal nerve stimulation were performed essentially as described (22, 25, 42). Glutamate iontophoresis was performed by using a sharp glass microelectrode inserted into the antennal lobe neuropil. Stimulation of LNs expressing the P2X2 receptor was achieved by pressure-ejecting ATP solution onto their somata. Paired recordings were performed in an ex vivo preparation to improve optical and steric access. See *SI Methods* for experimental genotypes and all other experimental details.

ACKNOWLEDGMENTS. We thank A. DiAntonio for anti-VGlut antibody, D. E. Krantz for anti-VGAT antibody, G. Miesenböck for *UAS-P2X2* flies, and members of the R.I.W. laboratory for feedback on the manuscript. This work was supported by National Institutes of Health research project Grant R01DC008174. W.W.L. is supported by an Howard Hughes Medical Institute (HHMI) International Research Fellowship and a Presidential Scholarship from Harvard Medical School. R.I.W. is an HHMI Early Career Scientist.

1. Daniels RW, Gelfand MV, Collins CA, DiAntonio A (2008) Visualizing glutamatergic cell bodies and synapses in Drosophila larval and adult CNS. *J Comp Neurol* 508(1):131–152.
2. Raghu SV, Borst A (2011) Candidate glutamatergic neurons in the visual system of Drosophila. *PLoS ONE* 6(5):e19472.
3. Das S, et al. (2011) Plasticity of local GABAergic interneurons drives olfactory habituation. *Proc Natl Acad Sci USA* 108(36):E646–E654.
4. Sudhakaran IP, et al. (2012) Plasticity of recurrent inhibition in the Drosophila antennal lobe. *J Neurosci* 32(21):7225–7231.
5. Xia S, et al. (2005) NMDA receptors mediate olfactory learning and memory in Drosophila. *Curr Biol* 15(7):603–615.
6. Wu CL, et al. (2007) Specific requirement of NMDA receptors for long-term memory consolidation in Drosophila ellipsoid body. *Nat Neurosci* 10(12):1578–1586.
7. Miyashita T, et al. (2012) Mg(2+) block of Drosophila NMDA receptors is required for long-term memory formation and CREB-dependent gene expression. *Neuron* 74(5): 887–898.
8. Das A, et al. (2011) Identification and analysis of a glutamatergic local interneuron lineage in the adult Drosophila olfactory system. *Neural Syst Circuits* 1(1):4.
9. Littleton JT, Ganetzky B (2000) Ion channels and synaptic organization: Analysis of the Drosophila genome. *Neuron* 26(1):35–43.
10. Parmentier ML, Pin JP, Bockaert J, Grau Y (1996) Cloning and functional expression of a Drosophila metabotropic glutamate receptor expressed in the embryonic CNS. *J Neurosci* 16(21):6687–6694.
11. Cully DF, Paress PS, Liu KK, Schaeffer JM, Arena JP (1996) Identification of a Drosophila melanogaster glutamate-gated chloride channel sensitive to the antiparasitic agent avermectin. *J Biol Chem* 271(33):20187–20191.
12. Masse NY, Turner GC, Jefferis GS (2009) Olfactory information processing in Drosophila. *Curr Biol* 19(16):R700–R713.
13. Wilson RI (2011) Understanding the functional consequences of synaptic specialization: Insight from the Drosophila antennal lobe. *Curr Opin Neurobiol* 21(2):254–260.
14. Chou YH, et al. (2010) Diversity and wiring variability of olfactory local interneurons in the Drosophila antennal lobe. *Nat Neurosci* 13(4):439–449.
15. Ramaekers A, Parmentier ML, Lasnier C, Bockaert J, Grau Y (2001) Distribution of metabotropic glutamate receptor DmGlu-A in Drosophila melanogaster central nervous system. *J Comp Neurol* 438(2):213–225.
16. Devaud JM, Clouet-Redt C, Bockaert J, Grau Y, Parmentier ML (2008) Widespread brain distribution of the Drosophila metabotropic glutamate receptor. *Neuroreport* 19(3):367–371.
17. Silbering AF, et al. (2011) Complementary function and integrated wiring of the evolutionarily distinct Drosophila olfactory subsystems. *J Neurosci* 31(38):13357–13375.
18. Stocker RF, Lienhard MC, Borst A, Fischbach KF (1990) Neuronal architecture of the antennal lobe in Drosophila melanogaster. *Cell Tissue Res* 262(1):9–34.
19. Cleland TA (1996) Inhibitory glutamate receptor channels. *Mol Neurobiol* 13(2): 97–136.
20. Raymond V, Sattelle DB, Lapied B (2000) Co-existence in DUM neurones of two GluCl channels that differ in their picrotoxin sensitivity. *Neuroreport* 11(12):2695–2701.
21. Barbara GS, Zube C, Rybak J, Gauthier M, Grünewald B (2005) Acetylcholine, GABA and glutamate induce ionic currents in cultured antennal lobe neurons of the honeybee, Apis mellifera. *J Comp Physiol A Neuroethol Sens Neural Behav Physiol* 191(9): 823–836.
22. Wilson RI, Laurent G (2005) Role of GABAergic inhibition in shaping odor-evoked spatiotemporal patterns in the Drosophila antennal lobe. *J Neurosci* 25(40):9069–9079.
23. Lima SQ, Miesenböck G (2005) Remote control of behavior through genetically targeted photostimulation of neurons. *Cell* 121(1):141–152.
24. Yaksi E, Wilson RI (2010) Electrical coupling between olfactory glomeruli. *Neuron* 67(6):1034–1047.
25. Olsen SR, Bhandawat V, Wilson RI (2007) Excitatory interactions between olfactory processing channels in the Drosophila antennal lobe. *Neuron* 54(1):89–103.
26. Shang Y, Claridge-Chang A, Sjulson L, Pypaert M, Miesenböck G (2007) Excitatory local circuits and their implications for olfactory processing in the fly antennal lobe. *Cell* 128(3):601–612.
27. Huang J, Zhang W, Qiao W, Hu A, Wang Z (2010) Functional connectivity and selective odor responses of excitatory local interneurons in Drosophila antennal lobe. *Neuron* 67(6):1021–1033.
28. Hamasaka Y, et al. (2007) Glutamate and its metabotropic receptor in Drosophila clock neuron circuits. *J Comp Neurol* 505(1):32–45.
29. McCarthy EV, et al. (2011) Synchronized bilateral synaptic inputs to Drosophila melanogaster neuropeptidergic rest/arousal neurons. *J Neurosci* 31(22):8181–8193.
30. Collins B, Kane EA, Reeves DC, Akabas MH, Blau J (2012) Balance of activity between LN(v)s and glutamatergic dorsal clock neurons promotes robust circadian rhythms in Drosophila. *Neuron* 74(4):706–718.
31. Clark DA, Bursztyn L, Horowitz MA, Schnitzer MJ, Clandinin TR (2011) Defining the computational structure of the motion detector in Drosophila. *Neuron* 70(6): 1165–1177.
32. Joesch M, Schnell B, Raghu SV, Reiff DF, Borst A (2010) ON and OFF pathways in Drosophila motion vision. *Nature* 468(7321):300–304.
33. Takemura SY, et al. (2011) Cholinergic circuits integrate neighboring visual signals in a Drosophila motion detection pathway. *Curr Biol* 21(24):2077–2084.
34. Chalasani SH, et al. (2007) Dissecting a circuit for olfactory behaviour in Caenorhabditis elegans. *Nature* 450(7166):63–70.
35. Scanziani M (2000) GABA spillover activates postsynaptic GABA(B) receptors to control rhythmic hippocampal activity. *Neuron* 25(3):673–681.
36. Wilson RI, Turner GC, Laurent G (2004) Transformation of olfactory representations in the Drosophila antennal lobe. *Science* 303(5656):366–370.
37. Olsen SR, Wilson RI (2008) Lateral presynaptic inhibition mediates gain control in an olfactory circuit. *Nature* 452(7190):956–960.
38. Root CM, et al. (2008) A presynaptic gain control mechanism fine-tunes olfactory behavior. *Neuron* 59(2):311–321.
39. Silbering AF, Galizia CG (2007) Processing of odor mixtures in the Drosophila antennal lobe reveals both global inhibition and glomerulus-specific interactions. *J Neurosci* 27(44):11966–11977.
40. Olsen SR, Bhandawat V, Wilson RI (2010) Divisive normalization in olfactory population codes. *Neuron* 66(2):287–299.
41. Isaacson JS, Scanziani M (2011) How inhibition shapes cortical activity. *Neuron* 72(2): 231–243.
42. Kazama H, Wilson RI (2008) Homeostatic matching and nonlinear amplification at identified central synapses. *Neuron* 58(3):401–413.

Supporting Information

Liu and Wilson 10.1073/pnas.1220560110

SI Methods

Fly Stocks. Flies were raised on standard cornmeal agar medium supplemented with potato food on a 12-h light/dark cycle at 25 °C. All experiments were performed on adult female flies 1–4 d after eclosion. The only exceptions were the experiments examining the effect of *GluClα* knockdown, where both control and RNAi flies were male. The genotypes used were as follows: Fig. 1 *B* and *C*, *OK371-Gal4/UAS-CD8:GFP*; Fig. 1 *D* and *E*, *pebbled-Gal4/+; UAS-nsyb:GFP/+*; Fig. 2, *OK371-Gal4/UAS-CD8:GFP*; Fig. 3 *A–D*, *GH146-Gal4,UAS-CD8:GFP*; Fig. 3 *D* and *E* and Fig. S1, *UAS-dicer2/Y;GH146-Gal4,UAS-CD8:GFP/+* (wild type) and *UAS-dicer2/Y;GH146-Gal4,UAS-CD8:GFP/ UAS-GluClα RNAi* (RNAi); Figs. 4 and 5, *OK371-Gal4,UAS-CD8:GFP/UAS-CD8:GFP;UAS-P2X2/+* (Glu-LN stimulation) and *UAS-CD8:GFP; UAS-P2X2/NP3056-Gal4* (GABA-LN stimulation); Fig. 6, *OK371-Gal4,UAS-CD8:GFP*; Fig. 7, *UAS-dicer2/Y;GH146-Gal4, UAS-CD8:GFP/+* (wild type) and *UAS-dicer2/Y;GH146-Gal4, UAS-CD8:GFP/UAS-GluClα RNAi* (RNAi); and Fig. S2, *GH146-Gal4,UAS-CD8:GFP*. Fly stocks were published as follows: *OK371-Gal4* (II) (1), *UAS-CD8:GFP* (II and III) (2), *pebbled-Gal4* (X) (3), *UAS-nsyb:GFP* (4), *GH146-Gal4* (II) (5), *UAS-P2X2* (III) (6), *NP3056-Gal4* (III) (7), *UAS-GluClα RNAi* (II) (8, 9), *UAS-dicer2* (X) (8). Stocks of *OK371-Gal4*, *UAS-CD8:GFP* (II and III), *UAS-nsyb:GFP*, and *UAS-dicer2* were obtained from the Bloomington *Drosophila* Stock Center. The *UAS-GluClα RNAi* insertion that we used in this study has been shown to substantially reduce *GluClα* RNAi levels in adult brain tissue (9), and we verified that it does not affect responses to iontophoresed GABA in these neurons (Fig. S1). However, it is difficult to completely exclude the possibility of off-target effects, given the lack of available alternative reagents for cross-validation. The *UAS-GluClα RNAi* insertion was obtained from the Vienna *Drosophila* RNAi Center (transformant ID 105754; sequence details available at http://stockcenter.vdrc.at).

Electrophysiological Recordings. In vivo whole-cell patch clamp recordings were performed essentially as described (10, 11). To perform recordings from Glu-LNs, the head was rotated 180° around the thin neck connective, so that the ventral side of the brain was facing upward and, therefore, accessible to visualization via the water-immersion objective above the preparation. The fly remained alive even when the head was rotated in this manner. The brain was perfused in external saline containing the following: 103 mM NaCl, 3 mM KCl, 5 mM *N*-Tris(hydroxymethyl) methyl-2-aminoethane-sulfonic acid, 8 mM trehalose, 10 mM glucose, 26 mM $NaHCO_3$, 1 mM NaH_2PO_4, 1.5 mM $CaCl_2$, and 4 mM $MgCl_2$ (osmolarity adjusted to 270–275 mOsm). The saline was bubbled with 95% O_2/5% CO_2 to pH 7.3. The internal solution for patch-clamp pipettes contained the following: 140 mM potassium aspartate, 10 mM Hepes, 1 mM EGTA, 4 mM MgATP, 0.5 mM Na_3GTP, 1 mM KCl, and 13 mM biocytin hydrazide. The pH of the internal solution was adjusted to 7.2, and the osmolarity was adjusted to ∼265 mOsm. In cases where antennal lobe projection neurons (PNs) and GABA-local neurons (LNs) were not labeled with GFP, they were identified based on the location and size of their somata, along with their distinctive intrinsic electrophysiological properties (11). Specifically, to record from PNs, we targeted our electrodes to the cluster of cell bodies immediately anterodorsal to the antennal lobe neuropil, which contains a pure population of uniglomerular PNs (12, 13). We confirmed that all these cells had small-amplitude action potentials (<12 mV), which is diagnostic of PNs (11). We also filled a subset of these cells with biocytin and verified that they were PNs based on their morphology. To record from GABA-LNs, we targeted our electrodes to the cluster of cell bodies lateral to the antennal lobe neuropil. This cluster contains both PNs and GABA-LNs (12, 13), but GABA-LNs are easily identifiable on the basis of their large action potentials (>24 mV), again as confirmed by biocytin fills (10, 11, 14). Glu-LN somata are located ventral to the antennal lobe, and so are in a distinctly different location from PN and GABA-LN somata. Glu-LN somata were always targeted for recording based on GFP expression (in *OK371-Gal4,UAS-CD8:GFP* flies), and in a subset of recordings, we used biocytin fills to verify that the GFP^+ cells we recorded from in this cluster were always antennal lobe LNs. Recordings were performed with an Axopatch 200B amplifier (Axon Instruments). Recorded voltages were low-pass filtered at 5 kHz and digitized at 10 kHz.

Odor Stimulation. Odors used were diluted 100-fold in paraffin oil and delivered via a custom-built olfactometer, which further dilutes the headspace of the odor vial 10-fold in air (15). Odor was delivered at a flow rate of 2.2 mL/min. Odor stimuli were applied for 2 s every 30 s, with five or six trials per stimulus. In one experiment, we observed odor-evoked firing rates that varied more than twofold over the course of the experiment, and we excluded this experiment from further analysis.

Histochemistry. In some experiments, the morphology of the recorded neurons was visualized after recording by incubating the brain with a fluorescent conjugate of streptavidin, as published (11). Immunohistochemistry was performed as described (10, 11). Primary antibodies were obtained from the following sources (with dilutions in parentheses): mouse nc82 from the Developmental Studies Hybridoma Bank (1:20), rat anti-CD8 from Invitrogen (1:200), rabbit anti-VGluT from A. DiAntonio (Washington University, St. Louis) (1:500; ref. 16), and rabbit anti-VGAT from D. E. Krantz (University of California, Los Angeles, CA) (1:200; ref. 17). Secondary antibodies (Invitrogen) were used at 1:250. To reconstruct neuronal morphology from biocytin fills, we hand-traced the skeletonized morphology with the Simple Neurite Tracer plugin in Fiji, using the Fill Out command to automatically generate a 3D volume, which we subsequently converted to a *z*-projection.

Glutamate and GABA Iontophoresis. For glutamate iontophoresis, a high-resistance sharp pulled glass pipette was filled with a solution of 1 M monosodium glutamate in water (pH 8). The pipette was placed in the antennal lobe neuropil, and glutamate was ejected by using a 10- to 20-ms negative current pulse applied with an iontophoresis current generator gated by a voltage pulse (Model 260; World Precision Instruments). A constant positive backing current was applied to retain glutamate in the pipette between ejections. The magnitude of the iontophoresis response depends on the placement of the pipette and the ejection current magnitude and duration, and these variables were adjusted in each experiment to ensure that the ejection artifact was small. (The artifact is visible as a downward deflection and flips symmetrically to become an upward deflection when the ejection pulse is inverted.) Because these adjustments are necessarily subjective, in the experiments comparing two genotypes (Fig. 3 *E* and *F*), the experimenter was blinded to genotype. For GABA iontophoresis, the glass pipette was filled with 250 mM GABA in water (pH 4.3). GABA was ejected by using a 20-ms positive pulse, and a negative backing current was applied to retain

GABA in the pipette between ejections. Tetrodotoxin (1 μM) was added to the bath in all iontophoresis experiments to block network activity.

Stimulation of LNs with ATP/P2X2. We used ATP/P2X2 to stimulate glutamatergic neurons because we found that expression of channelrhodopsin-2 under control of the *OK371-Gal4* driver produced lethality, likely due to basal activity of channelrhodopsin-2 in motorneurons. In our experiments using the ATP/P2X2 system (6), the ATP ejection pipette was filled with 10 mM MgATP in water and placed near the edge of the antennal lobe neuropil at the base of the ipsilateral antennal nerve (for Glu-LN activation), or at the dorsolateral edge of the antennal lobe neuropil (for GABA-LN activation). The ATP solution was pressure ejected for 10 ms at 6 psi by using a pneumatic device gated by a voltage pulse (PV820; World Precision Instruments). As a negative control, we recorded from Glu-LNs that lacked P2X2 expression (genotype *OK371-Gal4,UAS-CD8:GFP*) and confirmed that they were not depolarized by ATP. As an additional negative control, we also recorded from PNs and GABA-LNs in flies lacking the Gal4 driver (genotype *UAS-CD8:GFP*; *UAS-P2X2*) and confirmed that ATP ejection elicited a negligible response in these cells. However, if the ejection duration was prolonged beyond 10 ms, or if the pipette was buried in the antennal lobe neuropil, we observed a depolarization evoked by ATP pressure ejection in these control recordings.

Paired Recordings. Paired recordings were performed in an ex vivo preparation where the brain was removed from the head and immobilized on a coverslip. To target Glu-LNs in the paired recordings, we expressed GFP under the control of the *OK371-Gal4* driver. PNs and GABA-LNs were unlabeled but could be identified based on their soma location, soma size, and spike shape. The presynaptic cell was stimulated by injecting a 500-ms step of depolarizing current. The size of the step was adjusted to achieve depolarizations >30 mV in the stimulated cell. Current injections were repeated every 6 s for 30–60 trials. The response of the unstimulated cell was low-pass filtered at 50 Hz and averaged across trials. A pair was defined as connected if the response of the unstimulated cell was >0.3 mV. In a few cases, we defined a pair as connected even though the response was <0.3 mV, because the response was abolished by a neurotransmitter receptor antagonist (picrotoxin, CGP54626, or mecamylamine). In some pairs, we saw evidence of weak ephaptic coupling. These responses were small (typically <0.2 mV in the unstimulated cell) and had a latency and shape that was very similar to the voltage deflection in the stimulated cell, but in the opposite direction. They were not abolished by tetrodotoxin (1 μM).

Electrical Stimulation of Olfactory Receptor Neuron Axons. Electrical stimulation of the antennal nerve (in Fig. S2) was performed essentially as described (18). The ipsilateral antennal nerve was severed and drawn into a saline-filled suction electrode. A pair of 50-μs current pulses, 25 ms apart, was delivered to the nerve by using a current isolator (A.M.P.I.). We discarded trials in which there were unclamped spikes. We also discarded trials in which there were failures in either $EPSC_1$ or $EPSC_2$ (defined as events with an amplitude < 20% of the trial-averaged amplitude for that EPSC). Unitary EPSCs at this synapse are generally highly reliable in their trial-to-trial amplitudes, and so we interpret these failures as failures of axon recruitment, not failures of synaptic vesicle release. Consistent with this interpretation, we could sometimes obtain a more reliable recording by releasing and then reinserting the nerve into the suction electrode. Because of occasional large fluctuations in EPSC amplitude (likely due to fluctuating recruitment of axons), we only analyzed paired-pulse ratios over a run of trials where recruitment was stable. Specifically, paired-pulse ratios were measured over the maximum window of consecutive trials where the trial-to-trial coefficient of variation in $EPSC_1$ amplitude was less than 30%, where the minimum number of consecutive trials must be at least six. In these experiments, the iontophoretic ejection current began 400 ms before $EPSC_1$ and lasted 50 ms. This protocol ensured that the evoked EPSCs fell within the steady state of the postsynaptic outward current evoked by glutamate. The postsynaptic outward current evoked by glutamate iontophoresis was on average 6 pA, which was 22% of the average magnitude of $EPSC_1$ (27 pA). Current traces were low-pass filtered at 1 kHz before digitization at 10 kHz.

1. Mahr A, Aberle H (2006) The expression pattern of the Drosophila vesicular glutamate transporter: A marker protein for motoneurons and glutamatergic centers in the brain. *Gene Expr Patterns* 6(3):299–309.
2. Lee T, Luo L (1999) Mosaic analysis with a repressible cell marker for studies of gene function in neuronal morphogenesis. *Neuron* 22(3):451–461.
3. Sweeney LB, et al. (2007) Temporal target restriction of olfactory receptor neurons by Semaphorin-1a/PlexinA-mediated axon-axon interactions. *Neuron* 53(2):185–200.
4. Zhang YQ, Rodesch CK, Broadie K (2002) Living synaptic vesicle marker: Synaptotagmin-GFP. *Genesis* 34(1-2):142–145.
5. Stocker RF, Heimbeck G, Gendre N, de Belle JS (1997) Neuroblast ablation in Drosophila P[GAL4] lines reveals origins of olfactory interneurons. *J Neurobiol* 32(5): 443–456.
6. Lima SQ, Miesenböck G (2005) Remote control of behavior through genetically targeted photostimulation of neurons. *Cell* 121(1):141–152.
7. Chou YH, et al. (2010) Diversity and wiring variability of olfactory local interneurons in the Drosophila antennal lobe. *Nat Neurosci* 13(4):439–449.
8. Dietzl G, et al. (2007) A genome-wide transgenic RNAi library for conditional gene inactivation in Drosophila. *Nature* 448(7150):151–156.
9. Collins B, Kane EA, Reeves DC, Akabas MH, Blau J (2012) Balance of activity between LN(v)s and glutamatergic dorsal clock neurons promotes robust circadian rhythms in Drosophila. *Neuron* 74(4):706–718.
10. Wilson RI, Laurent G (2005) Role of GABAergic inhibition in shaping odor-evoked spatiotemporal patterns in the Drosophila antennal lobe. *J Neurosci* 25(40): 9069–9079.
11. Wilson RI, Turner GC, Laurent G (2004) Transformation of olfactory representations in the Drosophila antennal lobe. *Science* 303(5656):366–370.
12. Jefferis GS, Marin EC, Stocker RF, Luo L (2001) Target neuron prespecification in the olfactory map of Drosophila. *Nature* 414(6860):204–208.
13. Lai SL, Awasaki T, Ito K, Lee T (2008) Clonal analysis of Drosophila antennal lobe neurons: diverse neuronal architectures in the lateral neuroblast lineage. *Development* 135(17):2883–2893.
14. Yaksi E, Wilson RI (2010) Electrical coupling between olfactory glomeruli. *Neuron* 67(6):1034–1047.
15. Olsen SR, Bhandawat V, Wilson RI (2007) Excitatory interactions between olfactory processing channels in the Drosophila antennal lobe. *Neuron* 54(1):89–103.
16. Daniels RW, Gelfand MV, Collins CA, DiAntonio A (2008) Visualizing glutamatergic cell bodies and synapses in Drosophila larval and adult CNS. *J Comp Neurol* 508(1): 131–152.
17. Fei H, et al. (2010) Mutation of the Drosophila vesicular GABA transporter disrupts visual figure detection. *J Exp Biol* 213(Pt 10):1717–1730.
18. Kazama H, Wilson RI (2008) Homeostatic matching and nonlinear amplification at identified central synapses. *Neuron* 58(3):401–413.

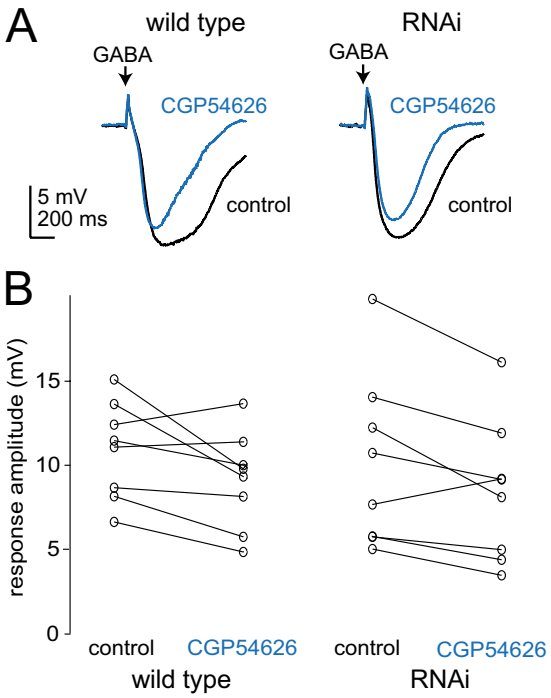

Fig. S1. *GluClα* knockdown does not affect PN responses to GABA. (*A*) Whole-cell recordings from an antennal lobe PN in a wild-type fly (*Left*) and a fly where the *GluClα* RNAi construct is expressed specifically in PNs (*Right*). A pulse of GABA in the antennal lobe neuropil (arrow) hyperpolarizes the PN in both cases. CGP54626 (50 μM) blocks the $GABA_B$ component of these responses, and what remains is the $GABA_A$ component (1). Note that the responses to GABA are similar in the two cells, as is the fractional block by CGP54626. (*B*) Group data showing responses to GABA iontophoresis in all experiments, before and after adding CGP54626. The percent inhibition by CGP54626 is not significantly different in the control and RNAi genotype ($P = 0.97$, student's *t* test). This result demonstrates that the RNAi construct is specific for *GluClα* and does not affect GABA receptors.

1. Wilson RI, Laurent G (2005) Role of GABAergic inhibition in shaping odor-evoked spatiotemporal patterns in the Drosophila antennal lobe. *J Neurosci* 25(40):9069–9079.

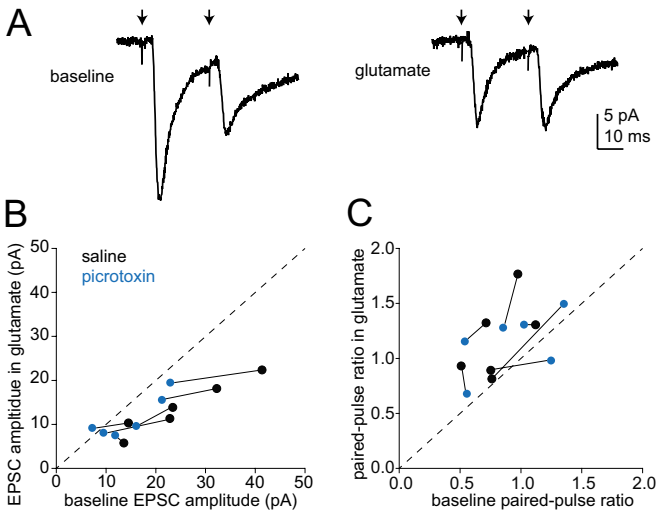

Fig. S2. Glutamate inhibits olfactory receptor neuron (ORN)-to-PN synapses. (*A*) A voltage-clamp recording from a PN shows EPSCs evoked by stimulation of ORN axons in the antennal nerve with a pair of electrical pulses (arrows). Glutamate iontophoresis inhibits EPSC amplitude. Glutamate also increases the relative size of EPSC2 to EPSC1, defined as the paired-pulse ratio (PPR = EPSC2/EPSC1). Traces are averages of 14 trials. (*B*) Summary of the effects of glutamate on EPSC1, where each symbol is a different experiment. Glutamate significantly inhibits EPSC1 amplitude ($P < 0.005$, two-way repeated-measures ANOVA, $n = 6$). The magnitude of inhibition by glutamate is significantly reduced by 100 μM picrotoxin (blue symbols, $P < 0.01$, two-way repeated-measures ANOVA), implying that GluCl contributes to this inhibition. Lines connect symbols corresponding to the same experiment. (*C*) Summary of the effects of glutamate on the paired-pulse ratio. Glutamate significantly increases PPR ($P < 0.05$, $n = 6$). An increase in PPR is classically associated with a decrease in presynaptic neurotransmitter release (1). However, picrotoxin does not significantly change the effect of glutamate on PPR ($P = 0.19$, two-way repeated-measures ANOVA). This result may reflect incomplete blockade of glutamate-gated chloride channels by picrotoxin (Fig. 3*D*) or an additional contribution to presynaptic inhibition from other glutamate receptors (e.g., a metabotropic glutamate receptor). In sum, these data show that the effects of iontophoretic glutamate on ORN-to-PN synapses are very similar to the effects of iontophoretic GABA (2, 3). This effect appears to be at least partly mediated by glutamate-gated chloride conductances, although metabotropic glutamate receptors may also contribute to presynaptic inhibition. Interestingly, GABAergic inhibition of neurotransmitter release from ORNs also appears to be mediated by both ionotropic and metabotropic GABA receptors (2).

1. Zucker RS, Regehr WG (2002) Short-term synaptic plasticity. *Annu Rev Physiol* 64:355–405.
2. Olsen SR, Wilson RI (2008) Lateral presynaptic inhibition mediates gain control in an olfactory circuit. *Nature* 452(7190):956–960.
3. Root CM, et al. (2008) A presynaptic gain control mechanism fine-tunes olfactory behavior. *Neuron* 59(2):311–321.